Numerical Analysis of Reinforcement Strains at Failure for Reinforced Embankments over Soft Soils

E.F. Ruiz, P.S. Hemsi, D.M. Vidal

Abstract. The use of geosynthetics as basal reinforcement in embankments constructed over soft soils provides technical and economic benefits by improving the stability of the structure, reducing horizontal displacements, homogenizing differential settlements, and reducing time of construction. An adequate design should include, however, more than routine limit equilibrium analyses, and should focus on understanding the soil-reinforcement interaction and mobilization of reinforcement strains during construction and with time, aspects that can be assessed with the use of finite elements simulations. This article presents the results of finite elements simulations for a hypothetical embankment over soft soil, applying the conceptual framework developed by Rowe & Soderman (1987), Rowe *et al.* (1995) and Hinchberger & Rowe (2003). Two approximate methods for obtaining the reinforcement allowable compatible strain at failure without the need for numerical simulations also are compared and discussed. The results in this article highlight the importance of assessing the mobilization of reinforcement strains during construction and taking into account soil-reinforcement interaction, given that reinforcement strains must be compatible with the soil system. An important implication, often overlooked in the past, is that the specification of geosynthetic materials for this application should be based on a minimum reinforcement stiffness modulus, *i.e.*, the ultimate strength of the material may not suffice as a specification parameter.
Keywords: embankment on soft soil, geosynthetic, numerical analysis, reinforcement strain mobilization.

1. Introduction

Limit equilibrium methods have become widespread as a technique for assessing the undrained stability of reinforced embankments on soft soils (Jewel, 1982; Rowe, 1984). However, the application of this approach requires a certain assumption on the reinforcement strain at failure. Using the ultimate tensile strength of the geosynthetic reinforcement in limit equilibrium analyses (*e.g.*, Michalowski, 1992) can lead to an overestimation of the short-term embankment stability, since reinforced embankments usually would have failed due to excessive displacements before the ultimate tensile strength of the reinforcement could be mobilized (Hinchberger & Rowe, 2003). This article presents a case study of evaluation of undrained stability for a hypothetical geosynthetic-reinforced embankment on soft soil where the shear strength increases with depth. The simulation of the ultimate limit state response is carried out by using numerical modeling (Bergado *et al.*, 1994, Palmeira *et al.*, 1998) with the finite elements method, following the conceptual framework presented by Rowe & Soderman (1987), Rowe *et al.* (1995) and Hinchberger & Rowe (2003).

A simplified methodology to ensure adequate end-of-construction (short term or undrained) stability by estimating the required minimum reinforcement stiffness modulus, J_{min}, is also described. Attention is given to the mobilization of reinforcement strains under this condition. Numerical results in terms of net embankment height, the development of contiguous plasticity of the soft soil, and allowable compatible strain are discussed. The objectives of this study are to develop comparisons between numerical results and two current approximate methods for obtaining reinforcement compatible strains, to develop a comparison between numerical results and traditional limit equilibrium results, and to discuss the implications of adopting an arbitrary reinforcement strain at failure on the stability of the embankment.

2. Materials and Methods

2.1. Embankment geometry

Figure 1 depicts the geometry adopted for this case study, representing a typical road embankment fill with design height, h = 2.30 m, crest width, b = 28.8 m, and side slopes 2(H):1(V), constructed over a soft clay foundation of D = 8.0 m depth, with undrained shear strength at the surface, S_{u0}, and a rate of increase of undrained shear strength with depth, ρ_c. An underlying permeable rigid stratum is assumed to occur below the soft clay layer.

2.2. Mesh discretization and initial conditions

Version 8.6 of the finite elements program *PLAXIS* (Plaxis, The Netherlands) (Brinkgreve & Vermeer, 2004) was adopted in this study to simulate the construction and

E.F. Ruiz, MSc., Civil Engineer, Instituto Tecnológico de Aeronáutica, Praça Mal. Eduardo Gomes 50, São José dos Campos, SP, Brazil. e-mail: fernando@huesker.com.br.
P.S. Hemsi, Ph.D., Associate Professor, Instituto Tecnológico de Aeronáutica, Praça Mal. Eduardo Gomes 50, São José dos Campos, SP, Brazil. e-mail: paulosh@ita.br.
D.M. Vidal, DSc., Associate Professor, Instituto Tecnológico de Aeronáutica, Praça Mal. Eduardo Gomes 50, São José dos Campos, SP, Brazil. e-mail: delma@ita.br.
Submitted on May 22, 2013; Final Acceptance on August 9, 2013; Discussion open until April 30, 2014.

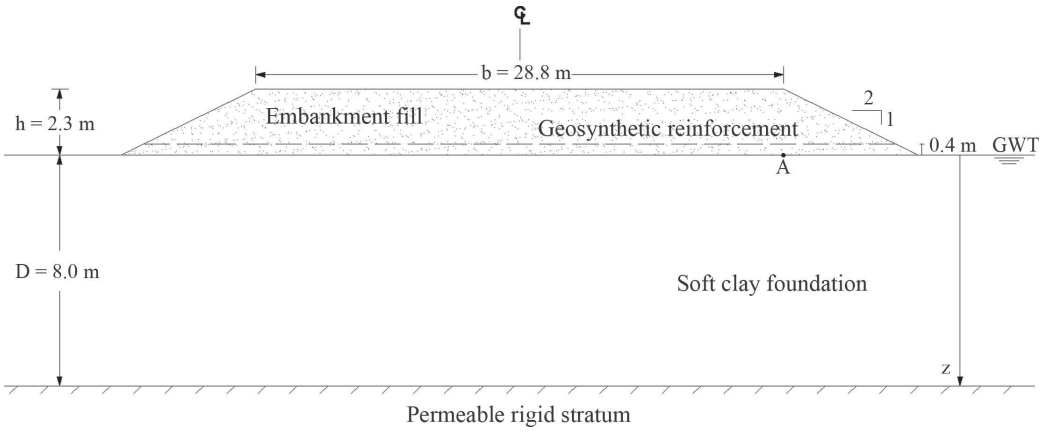

Figure 1 - Adopted embankment cross-section and foundation soil stratigraphy for the case study.

short-term stability of the reinforced embankment. A small deformation and plane-strain finite elements analysis was conducted for the assumed embankment cross-section (Fig. 1).

A typical unstructured finite element mesh (Fig. 2) with fifteen-node triangular elements with fine global coarseness was selected to discretize the embankment fill and foundation soil. Five-node *PLAXIS* line elements with input elastic axial stiffness were used to model the geosynthetic reinforcement. Appropriate mesh size and boundary conditions (*i.e.*, standard fixities option) were used to define the limits of the model and displacement restrictions around the cross-section.

Initial geostatic state of stresses was numerically calculated by adopting the K_o procedure. Since a phreatic level was defined at ground surface, the hydrostatic initial pore-water pressures were assessed automatically by the program. A rapid embankment construction was simulated by gradually turning on gravity on consecutive embankment layers in automatically defined thick lifts at a rate corresponding to instantaneous embankment construction (construction time is neglected). Due to the consideration of instantaneous construction, and short-term stability simulation, no soil water drainage was regarded in this case, *i.e.*, the foundation soil was assumed to undergo undrained loading.

The model lateral extension was defined based on a *PLAXIS* recommendation that the model should extend laterally a distance (each side) equal to four times the total embankment width (in this case, 4 x 38 m = 152 m to each side).

2.3. Constitutive models and soil parameters

The mechanical behavior of the foundation soft soil was modeled by using the Mohr-Coulomb constitutive model. Hence, it was assumed a soil with linear-elastic perfectly plastic stress-strain behavior, with fixed yield surface and non-associated plasticity rule. Anisotropy, progressive failure and more complex responses of the foundation soil were not modeled. The analyses were carried out in terms of total stresses, whereby the development of excess pore-water pressures is not calculated by the program. The set of undrained soft clay parameters adopted for this study is presented in the top part of Table 1. The parameters were selected on the basis of typical values for Baixada Santista's (São Paulo state lowland) hollocenic alluvial normally to slightly over-consolidated soft clays (Massad, 2009), which are similar to parameters in other studies (*e.g.*, Cappadoro *et al.*, 2007, Moraes, 2002). Also, the parameter set is similar to that used by Hinchberger & Rowe (2003).

A ratio $E_u/S_u = 125$ was selected for estimating the undrained Young's modulus of the soft clay, in agreement with the range reported by Duncan & Buchigani (1976), after a laboratory study carried out for a number of soft soils ($125 < E_u/S_u < 500$). The lower-end value chosen corresponds to a critical condition in terms of deformability.

Purely frictional granular soil was assumed to model the embankment fill, *i.e.*, the fill material was considered as being a pure sand. In order to represent the behavior of the sandy soil (*i.e.*, stress-strain hyperbolic relation, stress-level dependency of soil stiffness, shear and compression hardening), the Hardening soil model available in *PLAXIS*

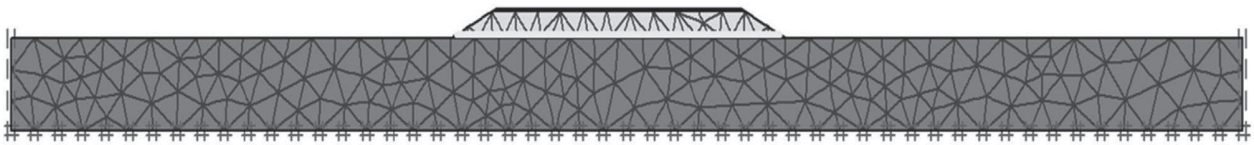

Figure 2 - Finite elements mesh based on triangular elements adopted for the numerical simulations.

was chosen (Schanz *et al.*, 1999, Brinkgreve & Vermeer, 2004). The assumed properties for the soil representing the embankment fill are shown in the bottom part of Table 1.

2.4. Interface parameters and reinforcement stiffness

The considered position for the geosynthetic reinforcement was 0.40 m above the fill/soft soil interface. For modeling, the interface elements representing the fill/reinforcement interface were assumed to follow an elastic perfectly-plastic model (Mohr-Coulomb criterion), and the interface parameter R_{inter} was chosen as being equal to 1.0, meaning that the interface fill/reinforcement was assumed to exhibit the same shear strength as the fill soil immediately surrounding the interface. The shear resistance of the soft soil-fill interface was assumed to be equal to the undrained shear strength of the foundation at the ground surface. The simplification $R_{inter} = 1.0$ has been used in Rowe & Soderman (1984), for example, and agrees with guidance from the *PLAXIS* manual.

The axial tensile stiffness (J) of the slender bar elements used to model the elastic behavior of the geosynthetic reinforcement was varied in different simulation cases, *i.e.*, from the value $J = 0$ (unreinforced embankment) to varying J values in different simulation cases, 300, 800, 500, 1000, 2000, 4000, 6000 and 8000 kN/m.

Table 1 - Geotechnical parameters assumed for the soft clay and the sand fill material.

Foundation soil	
Undrained shear strength at surface (S_{u0})	5.0 kPa
Rate of increase in undrained strength with depth, (ρ_c)	1.50 kPa/m
Total friction angle (φ)	0°
Saturated unit weight (γ_{sat})	15 kN/m^3
Undrained Poisson's ratio (ν_u)	0.48
Undrained Young's modulus (E_u)	$E_u/S_u = 125$
Coefficient of lateral earth pressure at rest (K'_0)	0.65
Embankment fill	
Effective internal angle of friction (φ')	37°
Effective cohesion intercept (c')	1.0 kPa
Compacted unit weight (γ_{bulk})	18 kN/m^3
Poisson's ratio for unloading-reloading (ν_{ur})	0.20
Secant triaxial stiffness modulus (E_{50})	25,000 kPa
Unloading-reloading stiffness modulus (E_{ur})	75,000 kPa
Oedometric stiffness modulus (E_{oed})	25,000 kPa
Coefficient of lateral earth pressure at rest (K'_0)	0.47
Power for stress-level dependency of stiffness (m)	0.50

2.5. Definition of the ultimate limit state

Ultimate limit states are associated with rotational and overall instability (as focused in this study), but also with other failure mechanisms, as depicted in Fig. 3 from the BS-8006 (2005).

These states are attained, for each specific mechanism, when disturbing forces or moments equal restoring forces or moments (available resistances). Margins and global factors of safety against attaining any limit state are provided by the use of partial load factors and partial material/resistance factors, producing design loads and design material parameters (BS-8006, 2005). For the case of reinforced embankments on soft foundation, Hinchberger & Rowe (2003) and Rowe & Taechakumthorn (2011) suggest the use of specific values for the partial factors, as shown in Table 2. Based on these partial factors, modified material parameters adopted to represent the ultimate limit state are also presented in Table 2.

3. Results and Discussion

3.1. Collapse height for the unreinforced embankment, H_c

By performing a conventional limit equilibrium analysis (slip circle, modified Bishop method) using the software *GGU Stability* (Civilserve GmbH, Germany), the collapse height for the embankment shown in Fig. 1 without reinforcement ($J = 0$) was estimated. In limit state design, the collapse height H_c corresponds to the height at which the overturning moment is equal to the restoring moment for factored soil parameters (*i.e.*, safety factor = 1.0). The collapse height, H_c, for the unreinforced embankment was

Table 2 - Ultimate limit state design parameters considered for this study.

Material parameters	Partial factors	Design values considered
Foundation soil		
Undrained shear strength at surface - $S_{u0} = 5.0$ kPa	$f_c = 1.3$	S_{u0}*= 3.85 kPa
Rate of increase in undr. strength w/ depth - $\rho_c = 1.50$ kPa/m	$f_c = 1.3$	ρ_c* = 1.15 kPa/m
Embankment fill		
Effective internal angle of friction - $\varphi' = 37°$	$f_\phi = 1.2$	φ'* = 32°
Compacted unit weight - $\gamma_{bulk} = 18$ kN/m^3	$f_\gamma = 1.1$	γ_{bulk}* = 20 kN/m^3

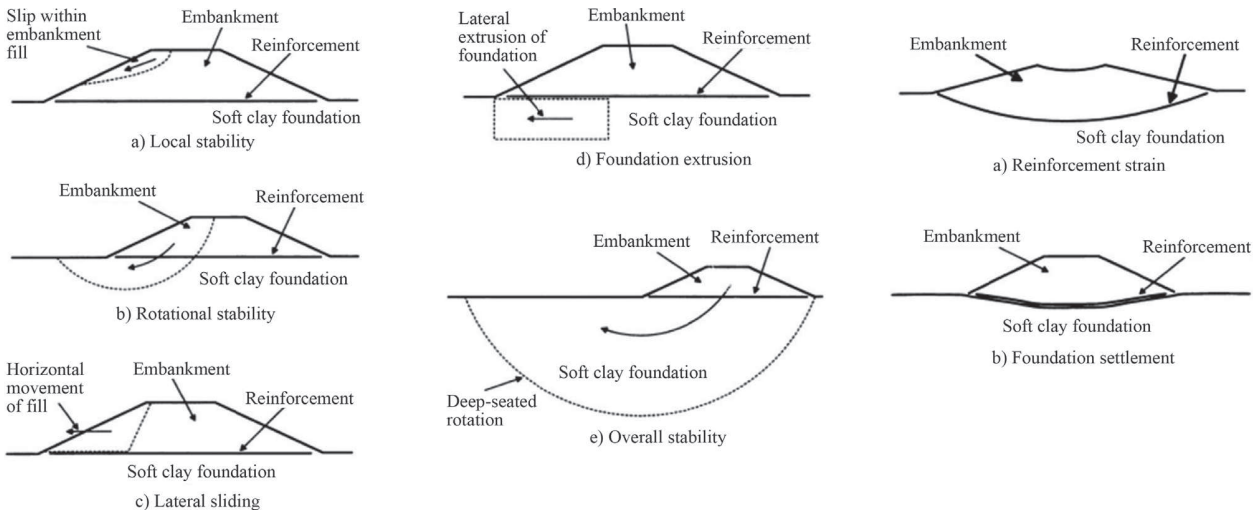

Figure 3 - Ultimate limit states for embankments on soft soils (modified from BS-8006, 2005).

found to be equal to 1.4 m. Since H_c is less than the required design height, h = 2.3 m, the use of a geosynthetic reinforcement is necessary in order to attain the additional fill height.

Figure 4 shows the critical failure circle from limit equilibrium superimposed to the displacement vector field from a complementary finite elements simulation of the same case.

3.2. Collapse height for the perfectly reinforced embankment, H_m

The theoretical maximum possible fill thickness for this case study, obtained for a perfectly-reinforced embankment (heavy reinforcement), H_m, was estimated based on plasticity limit analysis considering the problem of a rigid plate on soft foundation, as described by Almeida (1996). This maximum collapse height was estimated as being H_m = 2.50 m, for factored soil parameters. Since the required design height (h = 2.30 m) does not exceed H_m ($h < H_m$), the design embankment height may be achieved using embankment reinforcement. If $h > H_m$, soft soil improvement (*e.g.*, cement injection and mixing) or the use of a structural solution would be warranted.

3.3. Net embankment height and reinforcement allowable compatible strain

The instantaneous construction of the embankment was numerically simulated until collapse using the ultimate limit state design parameters in Table 2. The undrained stability of an embankment can be analyzed in terms of failure height of the structure. The failure height of a reinforced embankment can be defined as the height of fill at which the net embankment height ceases to increase. The net embankment height is defined as the fill thickness minus the vertical displacement caused by the undrained settlement of the soil (*i.e.*, fill height above the original ground surface). Thus, the failure height was obtained by plotting the net embankment height (*i.e.*, applied fill thickness minus the undrained vertical displacement of point "A" indicated in Fig. 1) *vs.* the total applied fill thickness. Figure 5 illustrates this plot, for the case study with a reinforcement J = 500 kN/m.

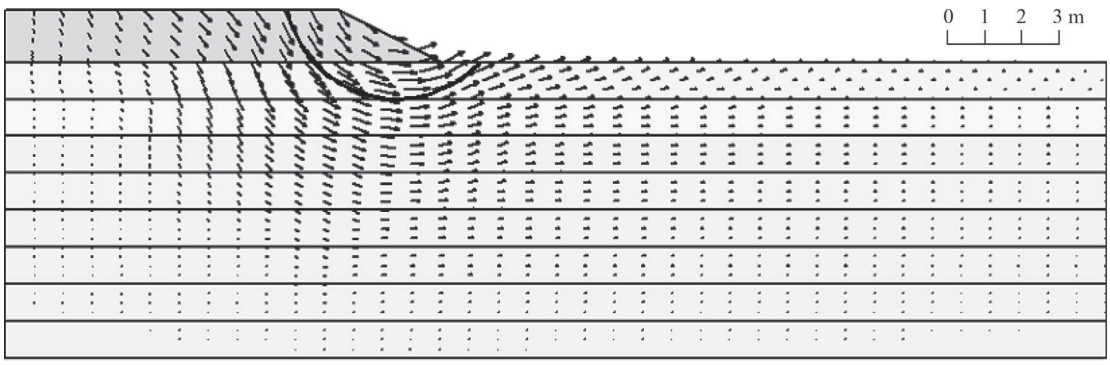

Figure 4 - Assessment of the embankment collapse height without reinforcement, H_c = 1.40 m, using limit equilibrium, superimposed to finite elements vectors.

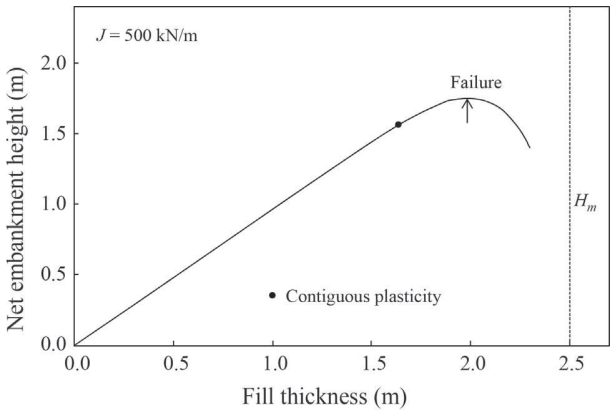

Figure 5 - Maximum net embankment height obtained by finite elements simulation of the case study with J = 500 kN/m.

As can be observed, the failure of the reinforced embankment due to excessive subsidence occurs at a fill thickness of about 1.98 m. Therefore, any additional fill placement beyond a thickness of 1.98 m will reduce the embankment performance without increasing the height of embankment fill above the original soft soil. For this reason, it is important to define the failure thickness of a reinforced embankment as the fill thickness corresponding to the maximum net embankment height. The degradation of the embankment performance can be explained as additional submersion of fill material into a plastic-state soft clay, with additional shearing and lateral movement (see Fig. 6). Rowe & Soderman (1987) defined contiguous plasticity as the point where there is general plastic failure within the soft soil in the region of a potential collapse mechanism (*i.e.*, the shear strength of the soil is fully mobilized along the potential collapse surface). For the unreinforced embankment, the maximum net fill height occurs at the onset of this limit. However, as indicated in Fig. 5 (see the contiguous plasticity point), for a reinforced embankment, the development of contiguous plasticity is only the first step towards failure, since some fill thickness can be supported by the reinforcement. Bergado *et al.* (2002) refer to the point of contiguous plasticity as primary failure. In Fig. 5, the fill thickness at the point of contiguous plasticity is ~ 1.64 m, which, in agreement with Bergado *et al.* (2002), occurs prior to failure due to excessive vertical displacement and complete degradation of performance.

In this study, the simulated zones of soft-soil plastification beneath the embankment were observed, particularly near the state of contiguous plasticity. The different configurations of soft-soil plasticity zones depend on the rigidities of both embankment/reinforcement and foundation soil, and the constitutive models (hardening soil for the embankment, in particular). For the condition of contiguous plasticity indicated in Fig. 5, the plastic zone within the foundation soil has become continuous resulting in an initial development of a potential failure plane.

Figure 6 shows the results of the numerical simulation in terms of the maximum mobilized reinforcement strains during embankment construction. At embankment failure, *i.e.*, a fill thickness of 1.98 m (Fig. 5), the maximum reinforcement strain (ε_f) is equal to 3.54% for J = 500 kN/m. The works of Rowe & Soderman (1987), Rowe *et al.* (1995) and Hinchberger & Rowe (2003) provided a quantifiable framework for recognizing the fact that in most cases (as shown here for the case study) the mobilized reinforcement strains are still low (*e.g.*, 3.54%) when the soil mass is already reaching failure. Several reinforcement geosynthetics have a similar stiffness, but significantly higher tensile strains at failure (> 3.54%), meaning that these reinforcements would not be fully loaded in the field before significant degradation of the soil.

Significant strains in the reinforcement only begin to accumulate after a significant plastification of the foundation soil, as indicated by the abrupt change in the slope of the curve of Fig. 6 after the point of contiguous plasticity. Beyond the point of contiguous plasticity of the soil, the reinforcement becomes the element that prevents collapse from taking place. Conversely, for low levels of embankment loading and soft soil in an elastic state, reinforcement strains are extremely small. The strains developed in the reinforcement for a given embankment height will largely depend on the height of embankment relative to that height at which contiguous plasticity occurs (Rowe & Soderman, 1987).

Past the maximum embankment height (failure, in Fig. 6), the placement of additional fill thicknesses will increase the plastification and degradation of the foundation soil, and be supported by additional elongation of the reinforcement, until a point of reinforcement collapse (9.76%, collapse point in Fig. 6).

The analyses were repeated for embankments with different reinforcement stiffness moduli, in three simulated cases, for J = 500, 1000 and 1500 kN/m, as shown in Fig. 7. From these results, the maximum net embankment height was found to increase with increasing the reinforcement

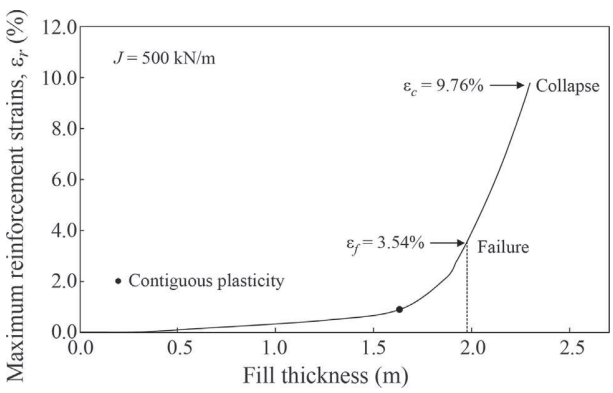

Figure 6 - Mobilized maximum reinforcement strains during embankment construction obtained by finite elements simulation of the case study with J = 500 kN/m.

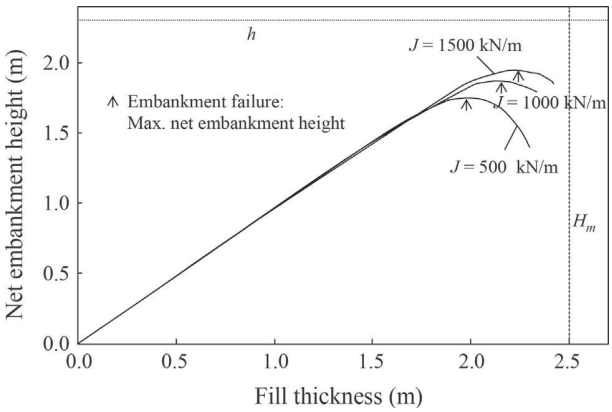

Figure 7 - Effect of varying *J* from 500 kN/m to 1000 and 1500 kN/m on the maximum net embankment height obtained by finite elements simulation of the case study.

stiffness modulus, for a given soil profile, with maximum net embankment heights of 1.98 m, 2.33 m , and 2.41 m, for *J* = 500, 1000, and 1500 kN/m, respectively. The effect of increasing *J* on the increase in maximum net embankment height diminishes with the magnitude of *J*, which is compatible with the existence of an H_m.

In addition, Fig. 8 presents the results in terms of mobilized reinforcement strains during embankment construction considering the three different reinforcement stiffness moduli, *J* = 500, 1000 and 1500 kN/m, for the simulated case. From the results, it is possible to observe that for the soft soil before contiguous plasticity the embankment strains are low and independent of reinforcement modulus. After contiguous plasticity, the reinforcement stiffness modulus becomes important, and different net embankment heights at failure are obtained for different values of *J* (Fig. 7). As shown in Fig. 8, the mobilized reinforcement strains decrease slightly with increasing values of *J*, from 500 to 1500 kN/m, for this case study. Hinchberger & Rowe (2003) identify two different ranges of behavior, a first "under-reinforced" embankment range characterized

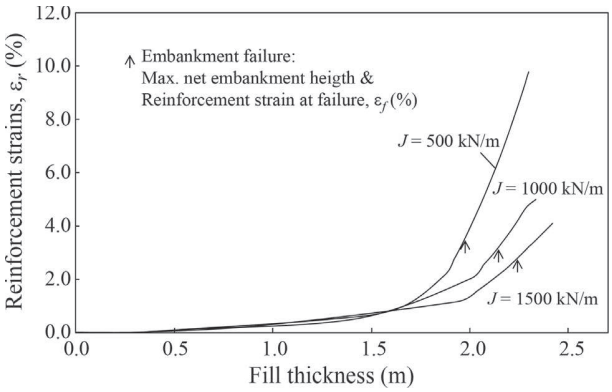

Figure 8 - Effect of varying *J* from 500 kN/m to 1000 and 1500 kN/m on the mobilized reinforcement strains obtained by finite elements simulation of the case study.

by mobilized reinforcement strains at failure (determined for the maximum net embankment height) that remain essentially constant for different values of *J*, and a second range of behavior characterized by reinforcement strains at failure that decrease with increasing reinforcement stiffness (*J*), such that the mobilized reinforcement force ($F = J \times \varepsilon$) approaches a constant value.

The results in Fig. 8 indicate that varying *J* from 500 to 1500 kN/m includes both ranges of behavior, *i.e.*, first "under-reinforced" behavior, and the second range of behavior. In order to better distinguish these two ranges, additional simulations were performed, extending the range in *J* from 300 up to 8000 kN/m. The obtained results are synthesized in Fig. 9. As expected, the maximum fill thicknesses at failure converge to the bearing capacity value given by plastic limit analysis. Based on the results, the range of "under-reinforced" embankment behavior was found to extend from *J* = 300 to 1000 kN/m, as indicated in Fig. 9.

Hinchberger & Rowe (2003) defined a reinforcement allowable compatible strain, ε_a, as being equal to the essentially constant strain occurring in the first range of behavior, *i.e.*, under-reinforced embankment. Since the reinforcement strains in the first range are assumed to be constant, the allowable compatible strain for the embankment in this case study was calculated as being equal to the average value of the strains obtained for *J* = 300 to 1000 kN/m, shown in Table 3.

3.4. Comparison with approximate methods

Generally, finite elements analyses remain costly as routine design procedure, which warrants the convenience of analytical calculations and charts. Hinchberg & Rowe (2003) introduced a chart for estimating the reinforcement allowable compatible strain simply, without requiring finite elements simulations to be performed.

For the unreinforced collapse height H_c = 1.40 m, and factored rate of increase in undrained shear strength ρ_c = 1.15 kPa/m, the allowable compatible strain for this

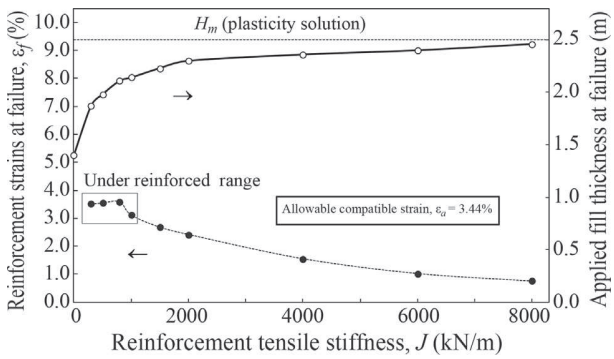

Figure 9 - Effect of varying *J* from 300 to 8000 kN/m on the mobilized reinforcement strains at failure (closed circles, see left-hand side scale) and applied fill thicknesses at failure (open circles, see right-hand side scale) obtained by finite elements simulation of the case study.

Table 3 - Calculation of a reinforcement allowable compatible strain for the embankment in this case study.

Stiffness modulus ("under-reinforced" range) J (kN/m)	Reinforcement strain at failure ε_f (%)
300	3.51
500	3.54
800	3.59
1000	3.12

Allowable compatible strain, ε_a = 3.44%.

case study results equal to 3.9% using the chart depicted in Fig. 10.

Also, Futai (2010) proposed, on the basis of numerical simulations, analytical correlations for estimating the reinforcement allowable compatible strains at failure for different scenarios. This proposal was developed by considering a proportional variable for the undrained shear strength of the foundation soil as the main parameter ($Su_0 + 7.5\rho$). The validation of the method was performed by comparing the calculated values and the measured strains of different instrumented embankments brought to failure.

For the factored soft-soil shear strength parameters in this study,

$$S^*_{u0} + 7.5\rho^*_c < 16.2 \text{ kPa} \quad (1)$$

and the correlation for allowable compatible strain to be used is (Futai 2010):

$$\varepsilon_a = 0.8\frac{S^*_{u0} + 7.5\rho^*_c}{9} \quad (2)$$

which results in an estimated value of reinforcement allowable compatible strain of 2.2%.

Thus, for this case study, estimation of the reinforcement allowable compatible strain using the simplified procedures resulted in either 15% overestimation (Hinchberg & Rowe, 2003) or 35% underestimation (Futai, 2010) with respect to the ε_a evaluated based on numerical analyses, as shown in Table 4.

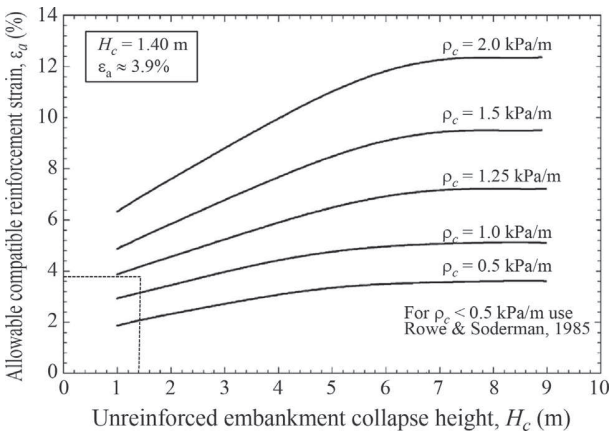

Figure 10 - Estimating the reinforcement allowable compatible strain for this case study using the chart by Hinchberger & Rowe (2003).

3.5. Minimum secant reinforcement stiffness modulus

The required reinforcement force, for the design fill thickness of 2.30 m, can be evaluated using limit equilibrium for a factor of safety of 1.0 for factored soil parameters as being equal to T_{ro} = 50 kN/m (modified Bishop method, software *GGU Stability*), as shown in Fig. 11.

Considering the reinforcement allowable compatible strain, ε_a, as being constant along the reinforcement length (*i.e.*, the reinforcement as being uniformly pulled), it is possible to evaluate the minimum required secant reinforcement stiffness modulus for design, as follows:

$$J_{\min} = \frac{\alpha_r T_{ro}}{\varepsilon_a} = 1.15 \times 50 \text{ kK/m} / 0.0344 = 1672 \text{ kN/m} \quad (3)$$

Adopting a reinforcement force correction factor, α_r = 1.15 (according to Hinchberger & Rowe, 2003).

Thus, the reinforcement minimum required secant stiffness modulus results from the combination of results obtained from limit equilibrium analyses and finite elements analyses (or the approximate methods shown in 3.4). The geosynthetic reinforcement to be considered for the embankment in this case study must meet the requirements of minimum secant stiffness modulus of 1672 kN/m over a strain range of 0 to 3.44%, and nominal ultimate strain greater than 3.44%.

3.6. Implications for design

Often, the necessary reinforcement force (T_{ro}) is known from limit equilibrium analyses but the magnitude of reinforcement strain is unknown. The fact that the reinforcement strain at which T_{ro} is mobilized must be also compatible with the deformation of the soft soil, is sometimes disregarded. The requirement for geosynthetic reinforcement selection must be a minimum secant stiffness modulus, and not a minimum tensile strength. Assume that for the case study described in this article an arbitrary reinforcement strain of 10% was considered, without taking into account strain compatibility with the soil, for the T_{ro} of 50 kN/m obtained from limit equilibrium for fill thickness

Table 4 - Comparison of reinforcement allowable compatible strain with approximated values obtained using two simplified procedures.

Approach	Allowable compatible strain, ε_a (%)
Finite Elements	3.4
Hinchberger & Rowe (2003)	3.9
Futai (2010)	2.2

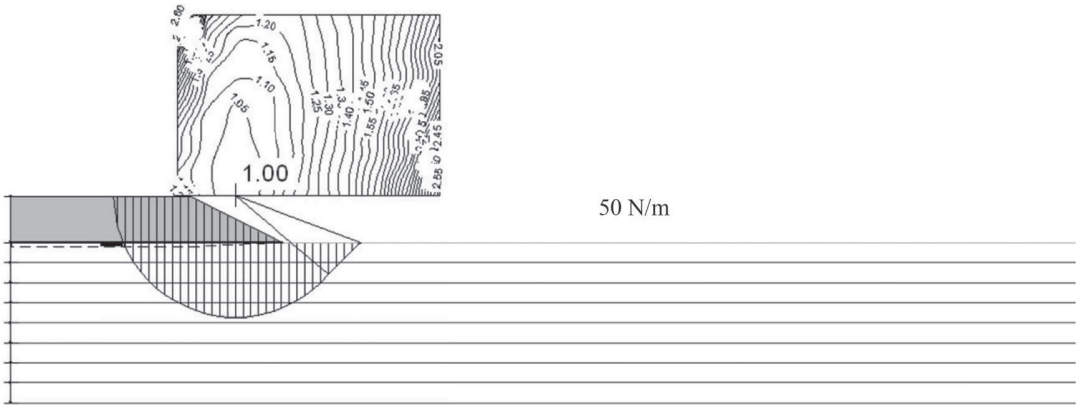

Figure 11 - Limit equilibrium stability analysis for factor of safety 1.0, allowing to estimate the required reinforcement force, T_{ro} (*GGU Stability*).

Table 5 - Differential behavior between 'minimum' and 'arbitrary' reinforcement stiffness.

Stiffness modulus, *J*	Applied fill thickness at failure (FEM)	Mobilized force at failure (FEM), $T_{mob\,f}$	Global factor of safety (LE)
J_{min} = 1672 kN/m	2.28 m	45.9 kN/m	1.21
$J_{arbitrary}$ = 500 kN/m	1.98 m	17.7 kN/m	1.02

FEM: finite elements method.
LE: limit equilibrium.

of 2.30 m. An arbitrary reinforcement stiffness modulus would be obtained, 500 kN/m.

As shown in Table 5, finite elements analysis of the embankment with a reinforcement with *J* = 500 kN/m indicates a mobilized reinforcement force at failure of only 17.7 kN/m. This force introduced into the limit equilibrium stability analysis results in an insufficient factor of safety (1.02).

Magnani *et al.* (2010) also described a similar type of behavior for the case study of a test embankment in Florianópolis, SC, Brazil, where the mobilized force in the reinforcement at failure was monitored by field instrumentation. The study verified that assuming a constant reinforcement force at failure and ignoring reinforcement strain may lead to an unconservative assessment of embankment stability.

4. Conclusions

Limit equilibrium analyses of the overall stability of reinforced embankments over soft soil can provide an estimate for a required reinforcement force for satisfactory factor of safety. However, an understanding of the soil-reinforcement interaction and mobilization of reinforcement strains during construction is critical for the correct definition of the geosynthetic reinforcement to employ. For a hypothetic embankment over soft soil considered in this study, the net embankment height, point of contiguous plasticity and reinforcement allowable compatible strain were studied following a previously defined theory. In addition, approximate methods for predicting the allowable compatible strain without the need for numerical simulations were verified, and one of the procedures overestimated the strain by 15%, whereas the other underestimated the strain by 35%. Finally, this article discussed the fact that the specification of geosynthetic materials for this application should be based on a minimum reinforcement stiffness modulus, instead of solely the ultimate strength of the material.

References

Almeida, M.S.S. (1996) Embankments on soft soils: from conception to performance evaluation. Ed. Universidade Federal do Rio de Janeiro, Rio de Janeiro, 216 pp (In Portuguese).

Bergado, D.T.; Long, P.V. & Murthy, B.R.S. (2002) A case study of geotextile-reinforced embankment on soft ground. Geotextiles and Geomembranes, v. 20:6, p. 343-365.

Bergado, D.T.; Long, P.V.; Lee, C.H.; Loke, K.H. & Werner, G. (1994) Performance of reinforced embankment on soft Bangkok clay with high-strength geotextile reinforcement. Geotextiles and Geomembranes, v. 13:6-7, p. 403-420.

Brinkgreve, R.B.J. & Vermeer, P.A. (2004) Reference Manual - Plaxis Finite Element Code for Soil and Rock

Analysis Version 8.6, Balkema, Rotterdam, The Netherlands.

British Standard BS-8006 (2005) Code of Practice for Strengthened/Reinforced Soils and Other Fills. British Standards Group, United Kingdom.

Cappadoro, A.P.; Porta, R. & Turello, D. (2007) Analysis of geogrids reinforced embankments over soft soils, numerical simulation. Graduate Thesis. Universidad Tecnológica Nacional, Santa Fe, Argentina, 275 pp (In Spanish).

Duncan, J.M. & Buchigani, A.L. (1976) An engineering manual for settlement studies. Geotechnical Engineering Report, Department of Civil Engineering, University of California at Berkeley, p. 94.

Futai, M.M. (2010) Considerations on the influence of the secondary consolidation and the use of reinforcement in embankments on soft soils. Post-Doctoral Thesis. University of São Paulo, São Paulo, 178 pp (In Portuguese).

Hinchberger, S.D. & Rowe, R.K. (2003) Geosynthetic reinforced embankments on soft clay foundations: predicting reinforcement strains at failure. Geotextiles and Geomembranes, v. 21:3, p. 151-175.

Jewell, R.A. (1982) A limit equilibrium design method for reinforced embankments on soft foundations. Proc. 2nd International Conference on Geotextiles, Las Vegas, v. 4, pp. 671-676.

Magnani, H.O.; Ehrlich, M. & Almeida, M.S.S. (2010) Embankments over soft clay deposits: contribution of basal reinforcement and surface sand layer to stability. Journal of Geotechnical and Geoenvironmental Engineering, v. 136:1, p. 260-264.

Massad, F. (2009) Marine soils from Santos region, characteristics and geotechnical properties. Ed. Oficina de Textos, São Paulo, p. 247. (In Portuguese).

Michalowski, R.L. (1992) Bearing capacity of nonhomogeneous cohesive soils under embankments. Journal of Geotechnical Engineering Division, v. 118:9, p. 1098-1118.

Moraes, C.M. (2002) Reinforced embankments over soft soils, numerical and analytical study. MSc. Thesis, Universidade Federal do Rio de Janeiro, Rio de Janeiro, p. 223 (In Portuguese).

Palmeira, E.M.; Pereira, J.H.F. & da Silva, A.R.L. (1998) Back-analyses of geosynthetic reinforced embankments on soft soils. Geotextiles and Geomembranes, v. 16:5, p. 273-292.

Rowe, R.K. (1984) Reinforced embankments: analysis and design. Journal of the Geotechnical Engineering Division, v. 110:2, p. 231-246.

Rowe, R.K. & Taechakumthorn, C. (2011) The interaction between reinforcement and vertical drains and effect of performance of embankments on soft ground. Soils and Rocks, v. 34:4, p. 261-275.

Rowe, R.K. & Soderman, K.L. (1987) Reinforcement of embankments on soils whose strength increases with depth. Proc. Geosynthetics 87, New Orleans, pp. 266-277.

Rowe, R.K.; Gnanendran, C.T.; Landva, A.O. & Valsangkar, A.J. (1995) Construction and performance of a full-scale geotextile reinforced test embankment, Sackville, New Brunswick. Canadian Geotechnical Journal, v. 32:3, p. 512-534.

Schanz, T.; Vermeer, P.A. & Bomeer, P.G. (1999) The Hardening Soil Model: formulation and verification. In: Beyond 2000 in Computational Geotechnics, 10 years of PLAXIS. Balkema, Rotterdam, The Netherlands.